Eur. Phys. J. D **42**, 359–368 (2007)
DOI: 10.1140/epjd/e2007-00038-4

THE EUROPEAN PHYSICAL JOURNAL D

Velocity selective optical pumping and repumping effects with counter and copropagating laser radiations for D_2 lines of rubidium

S. Chakrabarti[a], B. Ray, and P.N. Ghosh

Department of Physics, University of Calcutta, 92 A.P.C. Road, Kolkata-700009, India

Received 7 August 2006 / Received in final form 15 January 2007
Published online 23 February 2007 –

Abstract. The effects of a strong control or pump laser, counter propagating *or* copropagating with the probe beam, on the probe absorption spectra of ^{85}Rb and ^{87}Rb – D_2 transitions have been investigated inside a room temperature Rb vapour cell. In both cases a set of strong velocity selective resonance dips are observed at different velocities. Their movements across the Doppler broadened probe absorption profile have been studied for different lock frequencies of the control laser. These spectra are modified by optical pumping effects due to the presence of another hyperfine component of the ground state. A repumping laser, from the dark hyperfine component of the ground level transfers almost 75% of the atoms from the dark state to the pump probe cycle hence reducing the optical pumping effect. A numerical simulation is done to explain the observed spectra. The effect of a control laser on the Lamb dip spectrum of the probe laser has also been investigated. The control beam is used to improve the strength of a weak hyperfine dip on the Doppler broadened probe spectrum. The strength of the hyperfine dip increases by a factor of 3.2 in presence of the control laser. The observed dips show that pump-probe spectroscopy can be used as velocity selectors of atoms.

PACS. 32.80.Bx Level crossing and optical pumping – 32.70.-n Intensities and shapes of atomic spectral lines – 32.10.Fn Fine and hyperfine structure

1 Introduction

The dramatic advances in the resolution and sensitivity of laser spectroscopy of atoms have given a boost to the rapid developments in the fields of basic science of laboratory interest like laser cooling or Bose Einstein Condensation [1]. These achievements have also enabled technologies of a wide spectrum of new endeavors [2,3] that require extremely high precision for measurements upto umpteen significant digits. The necessity of identifying an isolated atomic transition and the locking of the laser frequency to a precise value offers several reasons for renewed effort to determine the individual transition frequencies. The major hindrance of laser frequency measurement is the Doppler broadening of spectral lines arising from the random atomic motion in the gas phase. Nevertheless laser spectroscopy affords methods to probe different velocity groups of atoms that interact with electromagnetic radiations with non-resonant transition frequencies.

Alkali atoms with non-zero nuclear spin exhibit hyperfine splitting of energy levels [4]. However the splitting in many cases is less than the Doppler width. Thus the hyperfine transitions are buried in the Doppler profile. The earliest and most established method of restoring these transitions is the standing wave Lamb-dip spectroscopy. In this technique the freely moving atoms are subjected to counter propagating laser radiations with the same frequency originating from a single source. One radiation creates a hole in the Boltzmann distribution curve of the lower level. When the other radiation comes across this hole a dip is observed in the absorption spectrum [5]. The dip has a narrow Lorentzian linewidth [6,7] depending on the collision broadening, laser linewidth, transit time broadening and natural linewidth. This simple story of Lamb dip at the resonance frequency observed for zero velocity atoms is further complicated when there are closely spaced levels and in fact, the spectroscopy of such systems is a prior objective of performing Lamb dip or saturation absorption spectroscopy of atoms. In the case of a single lower level and more than one close lying upper levels, in addition to the dips at the hyperfine transition frequencies, crossover resonance peaks are observed because the hole burnt by one radiation for a transition comes across the hole burnt by the radiation coming from the opposite direction on another transition [8]. The crossover resonance dip occurs at the mean frequency of the two transitions and has a similar linewidth and could often have a height comparable to the Lamb dip [9]. In the case of hyperfine spectra of atoms with one lower level and three upper levels three hyperfine and three crossover resonance

[a] e-mail: speclab_cu@yahoo.com

peaks are observed. This can make the resolution of the transitions often very tedious [10]. This situation is further complicated by the presence of a second lower hyperfine level for all D-lines of alkali atoms with $j = 1/2$, even though they are well separated so that there is no possibility of the transitions involving both the lower levels within a Doppler background. The problem originates from the fact that the atoms raised to the upper level from one lower level may decay back to the other lower level [11,12]. Thus the system is not closed and the atoms may be transferred to the other level by velocity selective optical pumping (VSOP). This lower state is a dark state and hence this may lead to a reduction of absorption [13], as the atoms of some velocity groups cannot take part in the absorption. As it is pointed out recently, except the closed transitions (e.g. $F = 3 \rightarrow F' = 4$ component of $^{85}\mathrm{Rb} - \mathrm{D}_2$ transition) all other transitions are not saturated, although Lamb dip spectroscopy in such cases is normally termed saturation absorption spectroscopy [11]. Lamb dip spectroscopy has the simplicity of using a single laser source, although the spectrum is marred by the presence of additional crossover resonances.

Recently pump probe spectroscopy for D_1 line of Na with two copropagating laser radiations showed that the hyperfine splitting can be very comfortably measured if one of the radiations (pump) is kept locked at a certain frequency within the Doppler background [14]. In this case there is no crossover resonance. Similar experiments have also been done with $\mathrm{Rb} - \mathrm{D}_2$ transitions [15]. Pump probe spectroscopy of rubidium forms the base for diverse experiments on Rb such as Electromagnetically induced transparency (EIT) [15], coherent population trapping (CPT) [16] and its application in constructing atomic clocks [17], four wave mixing, Sagnac interferometers [18] and lasing without inversion (LWI) [19] to name a few.

Motivated by the central role of the accurate knowledge of the hyperfine spectra of Rb, its use in frequency locking [19,20] for laser cooling experiments and the wide spectrum of experiments based on pump probe spectroscopy as listed above, we have studied different facets of pump probe spectroscopy in this work. The previous studies mostly concentrated on the so-called saturation spectroscopy with counter-propagating beams originating from the same laser or on pump probe spectroscopy with two co-propagating laser radiations.

In the first part of the work we study the pump probe spectroscopy with two independent tunable laser radiations traversing the gas atoms in the opposite directions. With the pump frequency kept locked to a particular frequency within the Doppler broadened curve of the $F = 3 \rightarrow F' = 2$, 3, 4 transitions of ^{85}Rb and the probe laser tuned across the same transitions we record both probe and pump powers. Velocity selective resonances predict the probe absorption to show new features with six transmission dips that show up as a broad and strong dip due to optical pumping in the observed Doppler broadened background. In the second part, to reduce the optical pumping effect by transferring the optically pumped atoms to the upper level, we use a repumper laser.

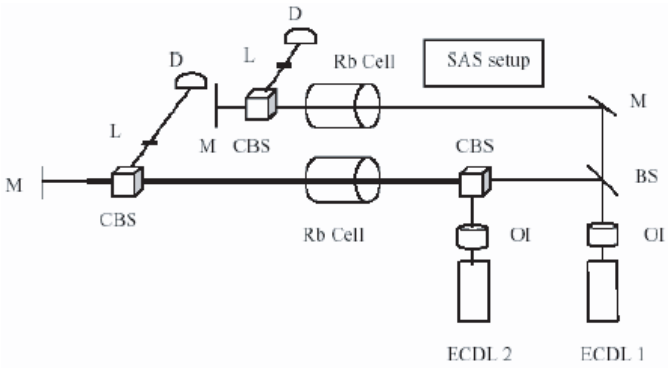

Fig. 1. Schematic representation of the experimental setup. ECDL: external cavity diode laser, OI: optical isolator, BS: beam splitter, CBS: cubical beam splitter, M: mirror, L: lens, D: detector and Rb Cell: rubidium vapour cell.

In the third part of the work we study the Lamb dip spectrum in the presence of a stronger coupling laser. For the counter propagating Lamb dip spectra we call the stronger component as pump and the weak counter propagating radiation as the probe. The stronger radiation from another source kept locked within the Doppler background is called control radiation. In such a system we can have three different types of features: (1) lamb dip spectrum with hyperfine and crossover resonance dips, (2) velocity selective resonance dips for the two copropagating laser radiations as reported earlier [21] and (3) velocity selective transmission dips for the two counter propagating beams as observed in the first part of the work. In this case when the control laser is on resonance with the hyperfine transition the Lamb dip for the hyperfine spectra becomes much stronger and is blown up compared to the crossover resonance peak. This dip gets broader because of saturation effect and optical pumping.

2 Experiment

The experiments are carried out inside a 5 cm long cylindrical room temperature vapour cell made of Pyrex glass having the window diameter 2.5 cm. The cell contains ^{85}Rb and ^{87}Rb isotopes in their natural abundances with no buffer gas. The cell is sealed at a pressure of 1 μtorr and its temperature is maintained at 299 ($\pm$0.1) K using a temperature controller. Three different narrow linewidth external cavity diode lasers (ECDLs) serve as sources for the pump (control), probe and repumping beams. An ECDL (from Sacher Laser Technik, Germany) in the Litthrow configuration produces the high power (95 mW/cm^2) pump beam while another ECDL (from New Focus, USA) in the Littman configuration produces the lower power (7.0 mW/cm^2) probe beam. After emanating from the ECDL the pump beam is split using a 70/30 beamsplitter. The transmitted part (30%) is sent through a saturated absorption spectrometer for locking the laser frequency (Fig. 1). The reflected part (70%) is expanded to form a circular beam of diameter 0.8 cm and is sent through

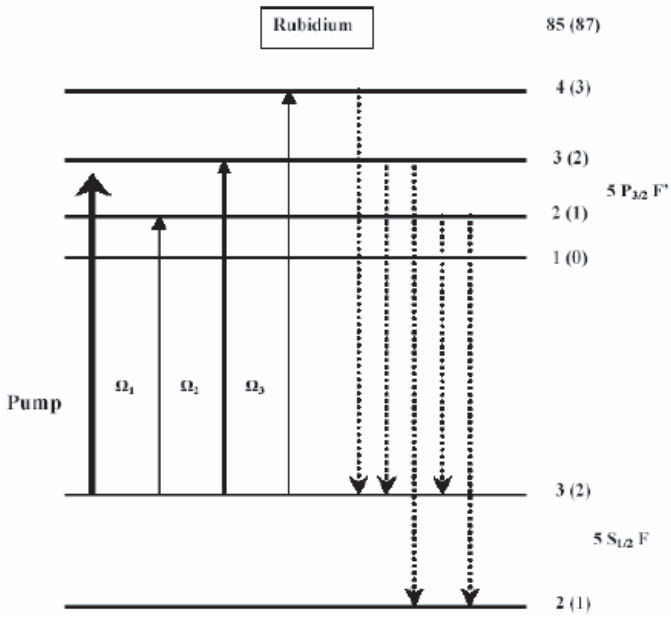

Fig. 2. Energy level diagram for ^{85}Rb and ^{87}Rb. Ω_1, Ω_2, Ω_3 represent the corresponding transition frequencies. The dotted lines represent the radiative decay channels for the atoms in the excited states.

the experimental cell. The probe beam (circular in shape) with diameter 0.15 cm intersects with the pump beam inside the experimental cell at a crossing angle less than 1° (10 mrad). Both the pump and probe beams have the same linear polarizations. The probe beam is focused onto a photodiode at a distance of one metre from the experimental cell such that there is appreciable spatial separation between the probe and pump beams. A digital storage oscilloscope (from Yokogawa, Japan) with a sampling rate of 200 kS/s recorded the output voltage from the photodiode. The pump laser piezo voltage is ramped using a very slow computer controlled ramp with ramp time 120 s across the $F = 3\ (2) \rightarrow F' = 2,\ 3,\ 4\ (1,\ 2,\ 3)$ transitions (Fig. 2) of ^{85}Rb (^{87}Rb) where from the different frequencies to be locked are selected and locked using a homebuilt proportional integrator differentiator (PID) electronic circuit having a long term lock stability of 1 MHz. The piezo voltage of the probe laser is ramped using a function generator with ramp frequency 30 Hz and ramp voltage 200 mV while recording the absorption profile of ^{85}Rb and 150 mV while doing the same for ^{87}Rb.

3 Observation and analysis

3.1 Effects of optical pumping on pump probe spectroscopy

In these experiments the pump laser is locked to several points (frequencies) across the $F = 3\ (2) \rightarrow F' = 2, 3, 4\ (1, 2, 3)$ transitions of ^{85}Rb (^{87}Rb) while the probe laser is scanned across the $F = 3\ (2) \rightarrow F' = 2, 3, 4\ (1, 2, 3)$ transitions (Fig. 2) of ^{85}Rb (^{87}Rb).

First the counter propagating probe and pump lasers are overlapped almost completely inside the vapour cell making a crossing angle less than 10 mrad while in the second experiment the pump and probe beams are aligned to copropagate almost completely making a crossing angle less than 10 mrad. In the next experiment the pump laser is retro reflected to simultaneously co and counter propagate with the probe beam such that a combination of the spectra obtained in the above two experiments is expected in this case.

A simulation is performed to reproduce the experimental results. Our simulation is based on the ^{85}Rb spectra. Similar results are expected for the 87 isotope too. The Gaussian widths of ^{85}Rb (524 MHz) and ^{87}Rb (518 MHz) are quite small compared to the separation between the 85 and 87 isotopes (∼1300 MHz). Hence for the purpose of simulation, we do not need to consider both the isotopes as there is no overlap between them.

The pump (control) laser leads to three transitions for three selected groups of velocities satisfying

$$\Omega_i = \omega_{pu}(1 + v_i/c) \quad \text{for} \quad i = 1, 2, 3. \tag{1}$$

Here, Ω_i represent the resonance frequencies (Fig. 2).

The tunable probe laser resonates with these velocity groups such that

$$\Omega_i = \omega_{pij}(1 \pm v_j/c) \tag{2}$$

where, $j\ (= 1, 2, 3)$ represents three different values of ω_p that resonate with Ω_i $(i = 1,\ 2,\ 3)$ for each of the values of v_i $(i = 1,\ 2,\ 3)$. The (+) and (−) signs correspond to the co and counter propagating pump probe geometries respectively.

The simulated spectra are obtained by using the Lorentzians

$$L(\omega) = \sum_{i=1}^{n} \left[\frac{A_i \Gamma}{(\omega - \omega_{0i})^2 + (\Gamma/2)^2} \right] \tag{3}$$

where n = number of transmission dips, $\omega - \omega_{0i} = k.\ v_i$, k are wave vectors, Γ is the natural linewidth, A_i is the normalization constant for the Lorentzian profile.

These simulated Lorentzians are convoluted with a normalized Gaussian profile $G(\omega)$ given by

$$G(\omega) = G_0 \exp\left[-\{c(\omega - \omega_0)/\omega_0 v_p\}^2\right] \tag{4}$$

where c is the velocity of light in air, v_p is the most probable velocity, G_0 is the normalization constant for the Gaussian profile, ω_0 is the central frequency of the Gaussian.

The resulting Doppler broadened simulated spectrum is obtained by convoluting the Lorentzian with the Gaussian as

$$I(\omega) = L(\omega)^* G(\omega). \tag{5}$$

The relative strengths of the Lorentzians have been considered while convoluting them with the Gaussian and have been estimated from the number of atoms lost by optical pumping corresponding to different velocities given by

$$\Delta N(\omega_L, v_z) = \Delta N^\circ(v_z) \left[1 - \frac{I/I_{sat}}{1 + I/I_{sat} + (2\Delta/\Gamma)^2} \right] \tag{6}$$

where $\Delta N = N_g - N_e$ is the difference in population between ground and excited states, ΔN° is the initial population difference, $\Delta = \omega_L - \omega_r$ is the laser frequency detuning, ω_L is the laser frequency, ω_r is the resonance frequency of transition, I is the laser intensity, I_{sat} is the saturation intensity for transition.

According to the calculations in all nine dips are expected for both the counter and copropagating conditions, with three dips corresponding to each of the velocities v_1, v_2 and v_3. For the counterpropagating case three pairs of dips have the same frequency. As a result instead of nine dips only six isolated dips are expected. Figure 3a displays the simulated Doppler free spectrum of the probe transmission against probe detuning. The dips corresponding to the different velocity group atoms are labeled in the spectrum. The 5 $^2S_{1/2}$ ground state for both the isotopes of Rb are split into two hyperfine components ($F = 2$ and 3) for ^{85}Rb and ($F = 1$ and 2) for ^{87}Rb. Owing to the presence of the second (lower) ground state hyperfine level the atoms raised to the upper excited levels namely F' (= 2, 3) for ^{85}Rb and F' (= 1, 2) for ^{87}Rb may decay back to this second ground state as also to the initial state. The atoms transferred to the other ground state due to velocity selective optical pumping (VSOP) cannot be raised to the higher excited states in absence of another pump field and are thus removed from the pump probe system. This lower ground state is thus called the dark state. The excited states from which the atoms may decay to the dark ground state are called open states and transitions to these states are called open transitions. From equation (1) it is clear that atoms having velocities v_1 and v_2 correspond to the open transitions Ω_1 and Ω_2 respectively (Fig. 2). Hence the transmission dips corresponding to the velocities v_1 and v_2 will have greater intensity due to optical pumping of atoms to the dark ground state compared to that due to the velocity v_3, which corresponds to the closed transition (Ω_3). A convolution of the Doppler free probe absorption spectrum with a Gaussian profile shows (Fig. 3b) only one strong power broadened transmission dip on the Doppler broadened simulated profile. Figure 3c represents the observed Doppler broadened probe transmission spectra for the $F = 3 \rightarrow F'$ (= 2, 3, 4) transition of ^{85}Rb when the pump laser counter propagates with respect to the probe laser. The locked pump laser frequency is indicated by an arrow on the Doppler broadened curve. The spectrum shows a single broad and intense transmission dip on the probe absorption profile at a probe frequency that is on the other side of the Doppler minimum compared to the pump frequency. If the pump is locked at the higher frequency side (as is the case in the figure) of the Doppler profile the dip occurs on the lower frequency side. The simulated convoluted spectrum (Fig. 3b) reproduces the experimentally observed spectrum (Fig. 3c) quite well. In contrast to the counter propagating case, for the copropagating pump probe configuration three dips are found to occur at the same frequency coinciding with the locked pump laser frequency. In this case seven independent dips are expected at different frequencies across the Doppler broadened probe absorption profile. Figure 4a shows the

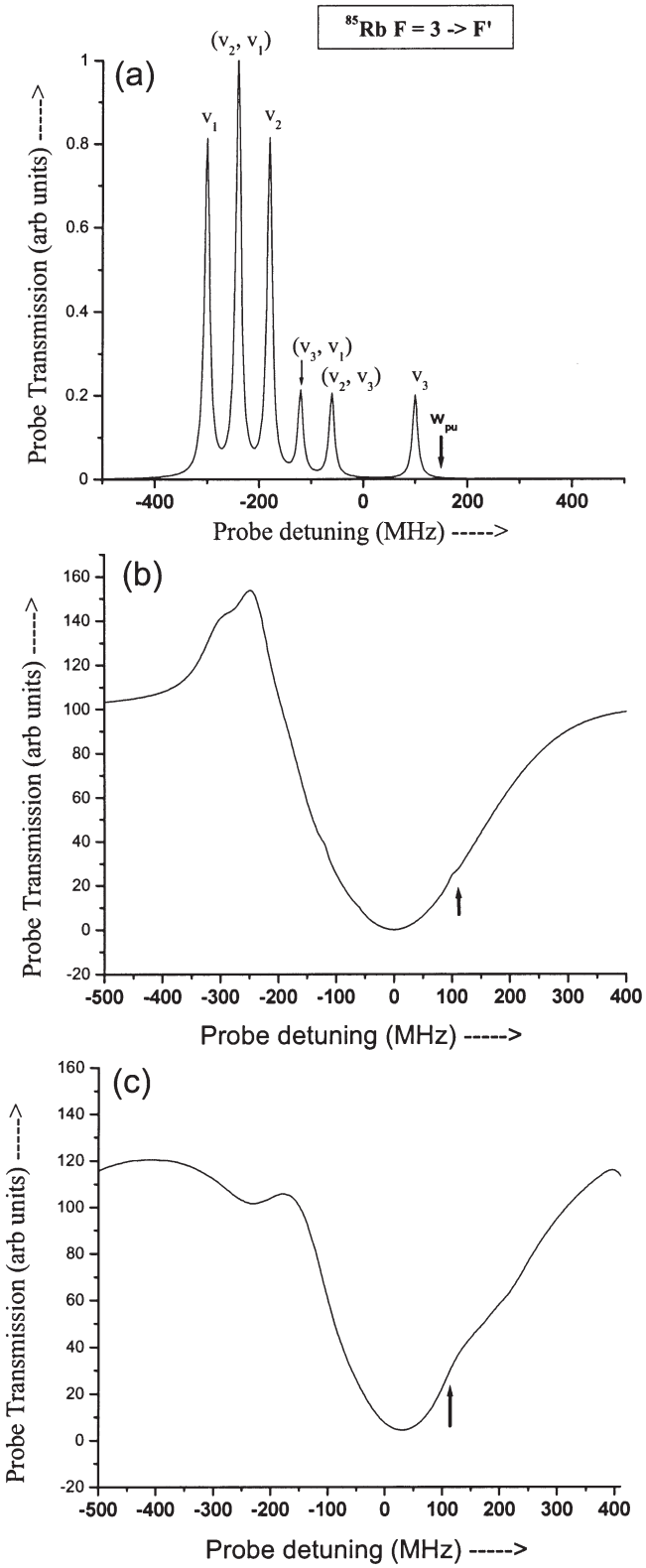

Fig. 3. Probe transmission spectrum for the $F = 3 \rightarrow F'$ (= 2, 3, 4) transition of ^{85}Rb (a) simulated Doppler free, (b) simulated Doppler broadened, (c) experimentally observed Doppler broadened spectrum. The counter propagating pump laser is locked to a frequency marked by arrow on the probe transmission profile. The dips corresponding to different velocities are marked.

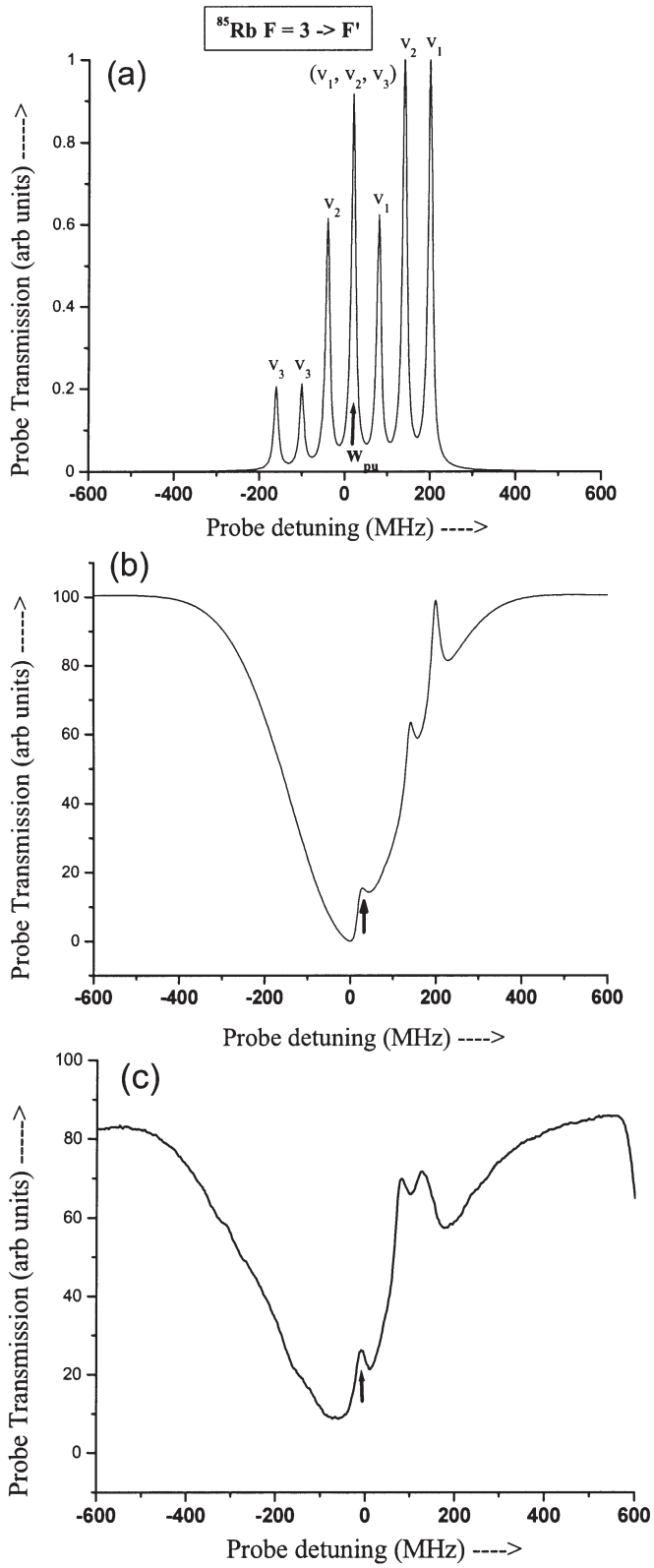

Fig. 4. Probe transmission spectrum for the $F = 3 \rightarrow F'$ (= 2, 3, 4) transition of ^{85}Rb (a) simulated Doppler free, (b) simulated Doppler broadened, (c) experimentally observed Doppler broadened spectrum. The copropagating pump laser is locked to a frequency marked by arrow on the probe transmission profile. The dips corresponding to different velocities are marked.

simulated Doppler free probe transmission profile for the copropagating pump probe system exhibiting the dips corresponding to different velocity groups. After convoluting with the Gaussian profile only three transmission dips are noticeable in the simulated spectrum (Fig. 4b). The two dips corresponding to the velocities v_1 and v_2 located on either side of the degenerate dip at the pump frequency could not be resolved as they were totally masked by the stronger power broadened dip at the pump frequency. The experimentally observed spectrum (Fig. 4c) resembles the simulated spectrum (Fig. 4b) with three dips.

Figure 5a gives the simulated Doppler free spectrum of the probe transmission profile in presence of simultaneous co and counter propagating pump fields. The dips corresponding to the co and counter propagating pump probe geometries are specified in the figure. The pump lock frequency is also indicated by an arrow. Figures 5b and 5c represent respectively the simulated and experimentally observed Doppler broadened probe transmission spectra for different lock frequencies of the pump laser for the corresponding case. The notable feature of the spectra is the manifestation of the two sets of transmission dips corresponding to the co and counter propagating pump probe arrangements and their crossing over when the pump frequency is shifted from the lower to the higher frequency range. As the pump frequency is moved the two sets of dips approach each other and then move away in opposite directions.

3.2 Optical pumping - effect of a repumping laser

Figure 6 represents the spectra when the counter propagating probe and pump signals are simultaneously recorded by two separate photo diodes and their outputs are fed to two channels of a digital oscilloscope in dual mode. The Doppler broadened curves represent the probe signal while the Doppler free ones represent the pump signal. The arrows indicate the pump lock frequencies. It is observed from the spectra (Fig. 6a) that when the pump laser is closer to the open transitions (Ω_1 and Ω_2) the strength of the transmission dip increases signifying greater loss of atoms to the dark ground state due to optical pumping whereas in Figure 6b the pump laser is away from the open transitions, showing smaller loss of atoms by optical pumping.

If a third laser is used to transfer atoms from the dark ground state to the excited states then the loss of atoms from the pump probe system could be controlled. With this objective in mind a third beam called hyperfine pumping or repumping beam derived from another ECDL is mixed with the counter propagating pump probe beams inside the vapour cell. The repumping field scans the $F = 2 \rightarrow F' = 1, 2, 3$ transitions of ^{85}Rb. This radiation brings back the atoms in the cycle of pump probe system and thus considerably reduces the VSOP dip (Fig. 7). In our experiment we have been able to transfer almost 75% of the atoms lost to the dark ground state by using a repumping laser of intensity 42 mW/cm^2. This study is very useful in many experiments where the atoms lost

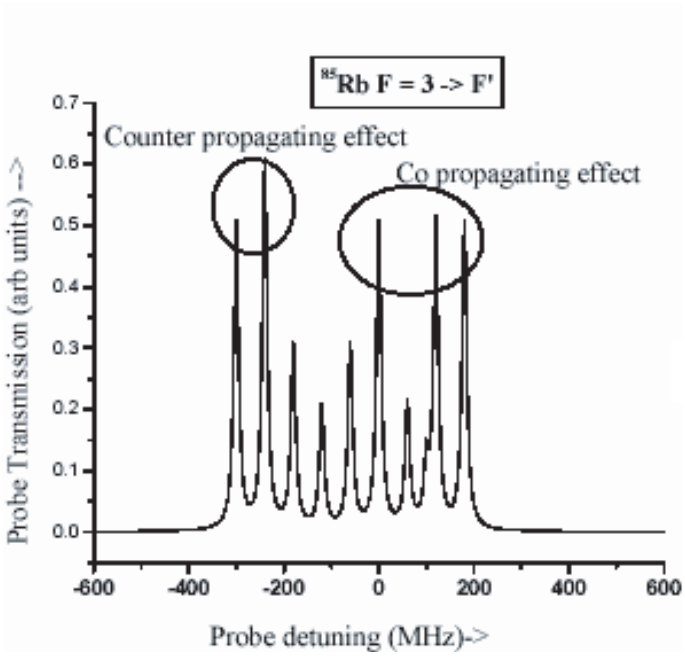

(a)

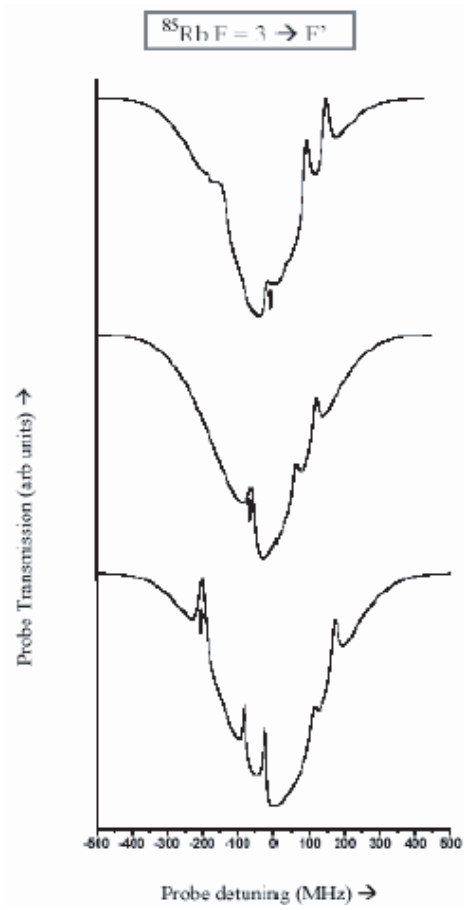

(b)

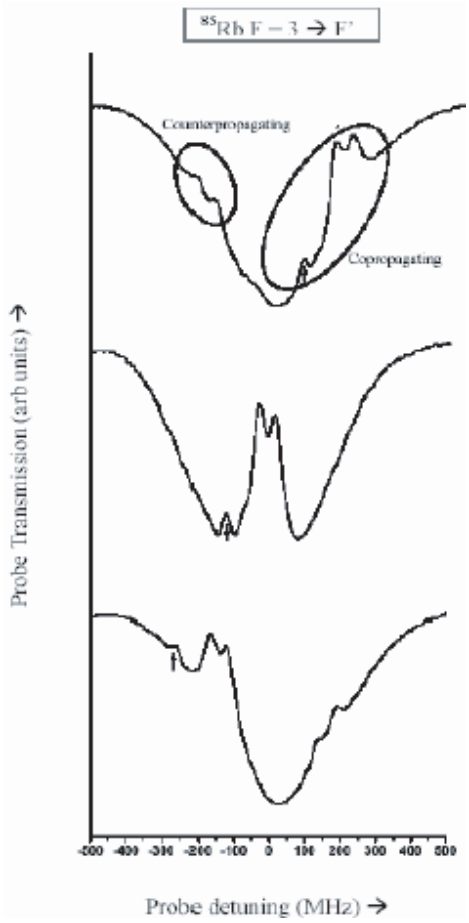

(c)

Fig. 5. Probe transmission spectrum in presence of simultaneous co and counter propagating pump laser fields for the $F = 3 \rightarrow F'$ (= 2, 3, 4) transition of ^{85}Rb (a) simulated Doppler free, (b) simulated Doppler broadened, (c) experimentally observed Doppler broadened spectrum. The copropagating pump laser is locked to a frequency marked by arrow on the probe transmission profile. The dips corresponding to different velocities are marked.

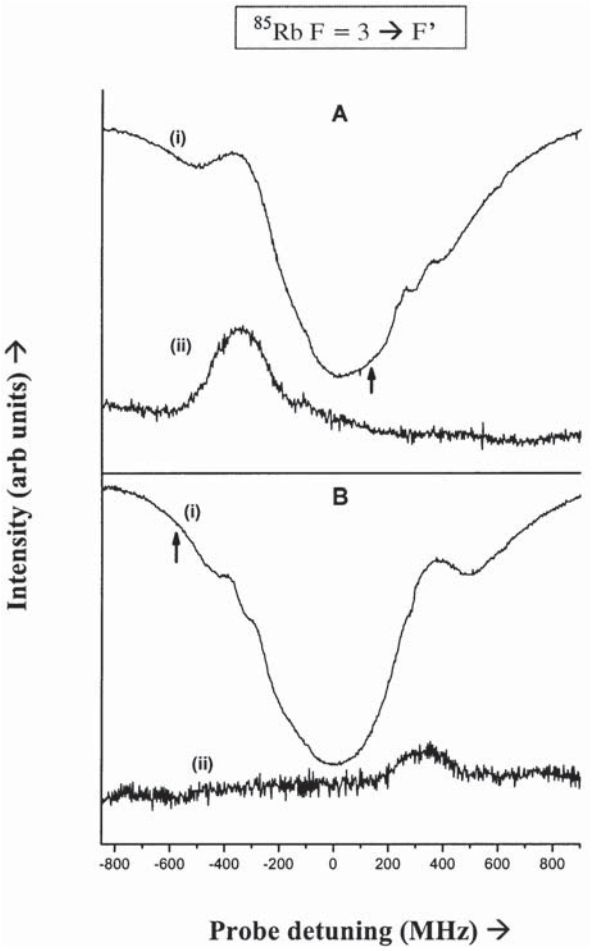

Fig. 6. Spectra when the counter propagating probe and pump signals corresponding to the $F = 3 \rightarrow F'$ (= 2, 3, 4) transition of ^{85}Rb are simultaneously recorded. A(i) gives the Doppler broadened probe signal and A(ii) gives the Doppler free pump signal, when the pump frequency (marked by arrow) is locked in between the open transitions $F = 3 \rightarrow F'$ (= 2) and $F = 3 \rightarrow F'$ (= 3). B(i) gives the Doppler broadened probe signal and B(ii) gives the Doppler free pump signal, when the pump laser is locked at a frequency (marked by arrow) red detuned by 500 MHz from the $F = 3 \rightarrow F'$ (= 2) transition.

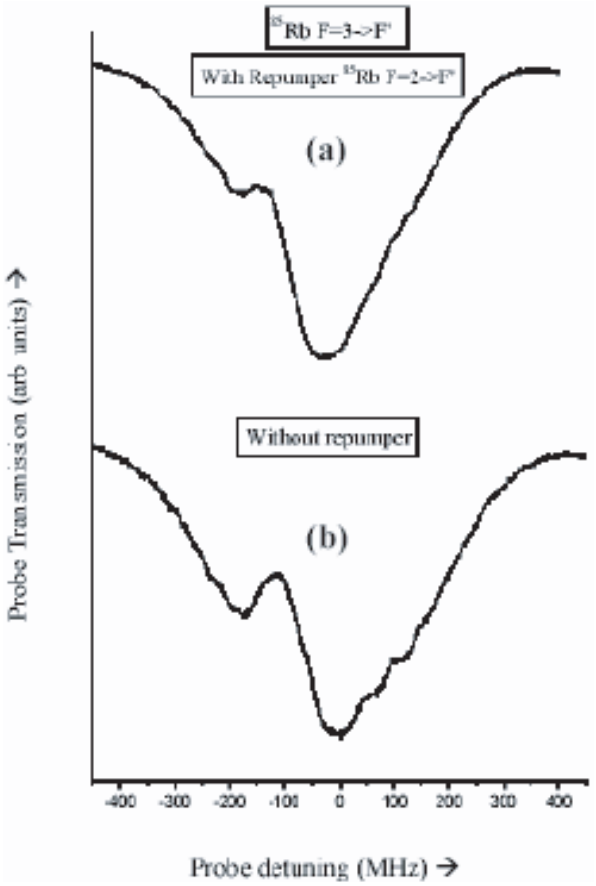

Fig. 7. Doppler broadened probe transmission spectra for ^{85}Rb with a counter propagating pump probe configuration in presence (a) and absence (b) of a repumping laser scanning the $F = 2 \rightarrow F'$ (= 1, 2, 3) transition of ^{85}Rb.

in the dark hyperfine state(s) can be brought back to the cycle.

3.3 Effect of pump laser on the Lamb dip spectrum of probe laser

Figure 8 presents the spectra of ^{85}Rb with counter propagating laser radiations leading to Lamb dip and crossover resonances of the probe beam in the presence of a control laser locked at different frequencies within the Doppler broadened profile. In absence of the control laser the standard hyperfine and crossover resonance dips are observed. In presence of the control laser the dips are modified by hyperfine pumping effects changing their relative strengths. When the control frequency is shifted along the Doppler profile of the probe absorption curve the strong VSR dips arising from the counter propagating beam and the weaker VSR dips arising from the copropagating beams move towards each other. When the control frequency resonates with one of the hyperfine transitions a strong dip is observed at this frequency of the Lamb dip spectra of the probe. This enhances the hyperfine dip such that it surpasses the height of the crossover resonance dip, which remains unperturbed in the Lamb dip spectrum (Fig. 8). An accurately locked control laser can in this way enhance the hyperfine transition, which is otherwise weak. However the dip has much larger linewidth due to power broadening and optical pumping. Such a spectrum is not saturated since the atoms of a wide range of velocity groups are transferred to the other lower hyperfine level by the optical pumping.

Table 1 gives the relative strength and width of the $F = 3 \rightarrow F' = 4$ hyperfine transition in the Lamb dip spectrum of ^{85}Rb in presence and absence of the control laser. The natural linewidth of the hyperfine transition is mentioned in place of the calculated width in absence of control laser. However considering power broadening effects it was estimated to be 12 MHz. The strengths have been normalized with respect to the experimentally

Table 1. Gives the relative strengths and widths of a hyperfine transmission dip in presence and absence of a control laser.

	Relative strength of transmission dip when control laser is		Width of transmission dip when control laser is	
	present	absent	present	absent
calculated	6.38	1.46	45 MHz	6 MHz
experimental	3.2	1.0	36 MHz	15 MHz

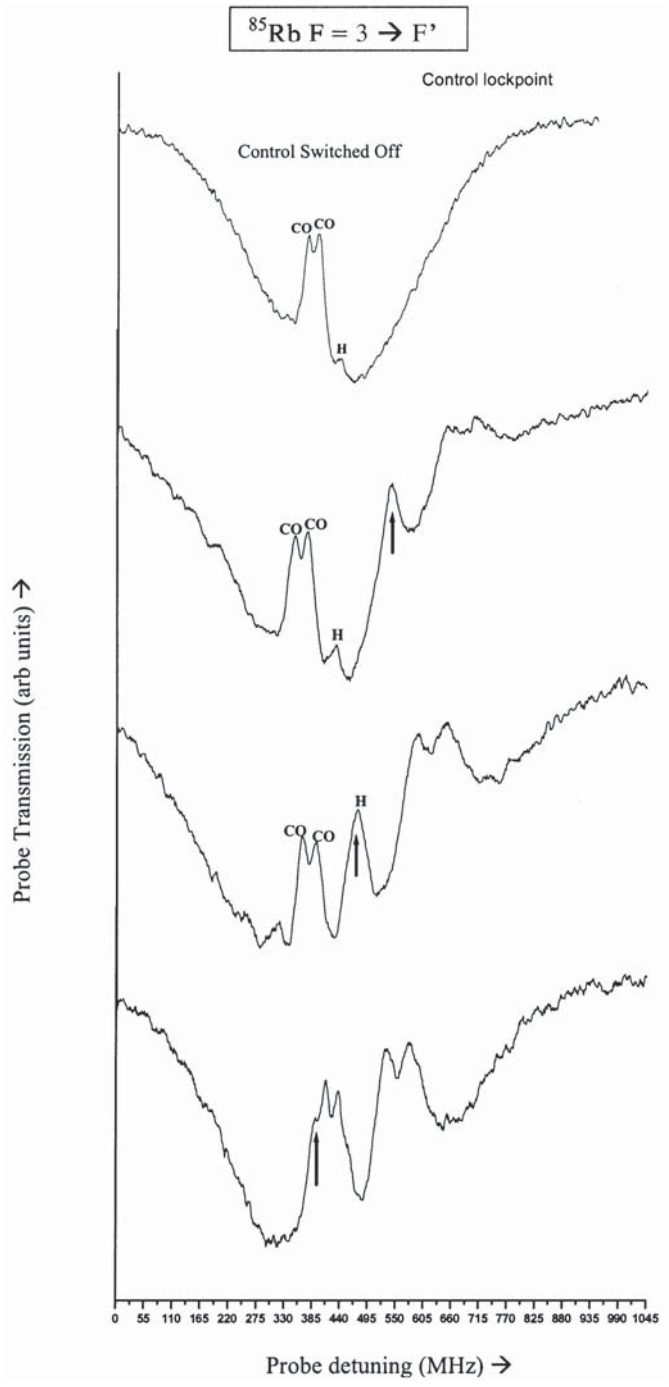

Fig. 8. Doppler broadened Lamb dip spectra of the probe laser scanning the $F = 3 \rightarrow F'$ (= 2, 3, 4) transition of ^{85}Rb in presence of a control laser simultaneously co and counter propagating with the probe. COs represent the crossover resonances while H represents the hyperfine resonance.

observed strength in absence of the control laser taken as 1.0. It is shown that the increase in the strength of the hyperfine transition in presence of the control laser is 3.2 times that in absence of the control field.

4 Discussions

This work reports for the first time spectroscopy with counter propagating pump probe beams derived from two different laser sources. The strong pump beam modifies the Doppler broadened probe absorption as expected. Unlike the conventional saturation absorption spectroscopy [11,13], where both the pump and probe beams (obtained from the same source) are scanned across the $F = 3 \rightarrow F'$ (= 2, 3, 4) transition manifold of ^{85}Rb, here the pump laser is kept locked to specific frequencies on the $F = 3 \rightarrow F'$ (= 2, 3, 4) transition of ^{85}Rb and the probe laser is scanned across the Doppler profile. In the conventional saturation absorption spectroscopy the pump and probe beams being produced from the same laser source interact simultaneously only with the zero velocity atoms at different resonance frequencies. In our experiment the pump and probe beams derived from different laser sources interact with non–zero velocity group of atoms corresponding to the different hyperfine resonance frequencies. This enables us to probe various velocity groups of atoms and isolate them from the rest of the atoms in the distribution. In the energy level configuration considered here six non degenerate dips are predicted and the observed dips are found to lie on the opposite sides of the Doppler profile with respect to the pump frequency. This is in contrast with the case of the pump beam co propagating with the probe laser that predicts seven velocity selective resonance dips across the Gaussian profile of the probe, where one of these dips always coincides with the pump frequency. Instead of the predicted seven dips only three could be observed to have sufficient strength. These dips move across the Gaussian profile of the probe along with the pump laser frequency when it is changed [22]. In the counter propagating case the movement is in a direction opposite to that of the pump laser frequency. The dips mentioned above for both the co and counter pump probe alignments are caused by holes created in the probe ground state due to depletion of atoms belonging to certain velocity groups that are continuously raised to higher excited states by the pump field. These atoms again decay back to the ground state. Thus a state of dynamic equilibrium is reached. However due to the presence of another hyperfine component of the ground state some of the atoms raised by the pump to

the excited states decay to this dark ground state where from they can no longer be excited by the pump laser and are lost from the emission absorption cycle. The decay from the excited states to the dark ground state leads to a much broader peak and thus the dips cannot be resolved. Some of the previous works [11,13] also investigated the optical pumping effects produced due to the presence of the dark hyperfine component of the ground state. There the authors commented on the modification of the saturated absorption spectra by optical pumping, however they did not confirm the extent of modification experimentally. We have used a third laser from the $F = 2\ (1) \rightarrow F'$ of ^{85}Rb (^{87}Rb) called the repumping laser to replenish the loss of atoms from the system to the dark ground state $F = 2\ (1) \rightarrow F'$ of ^{85}Rb (^{87}Rb). As a result the strong velocity selective resonance dips caused by the optical pumping effects become weaker in presence of the repumping laser field. The repumping beam reduces the optical pumping effects by almost 75%. Thus using a repumping beam one can estimate the loss of atoms from the ground state due to saturation by the strong pump field and due to optical pumping to the other dark ground state.

A simulation of the spectra considering a pump beam co and counter propagating with the probe field reproduces the experimental observations. The effects of optical pumping are taken into account. This is done by calculating the magnitude of velocities of the atoms that participate in the optical pumping process. The number of atoms involved in the optical pumping phenomenon corresponding to these velocities is then estimated. The number of atoms thus calculated gives an idea of the strength of optical pumping at different frequency positions across the Gaussian distribution. This fact is incorporated in the simulation by assigning greater (varying) strengths to the transitions involved in optical pumping. The Doppler free simulated spectra show seven dips for copropagating situation and all six dips for the counter propagating case. However after convolution with Doppler profile the simulated spectra revealed only a few dips in agreement with the experimental observation.

In this work we also try to manipulate the strength of hyperfine transmission dips, obtained by conventional Lamb dip spectroscopy, by using a higher intensity control laser. We also carried out Lamb dip spectroscopy of the probe beam for the ^{85}Rb atom in presence of a strong control laser co and counter propagating with it. Two strong crossover dips and one weak hyperfine dip could be resolved from the Doppler broadened Gaussian profile in absence of the control field. When the control laser frequency is locked to the hyperfine transition the hyperfine dip gets greatly enhanced and becomes stronger than the crossover dips. However due to optical pumping the hyperfine dip broadens in width in presence of the control field. Thus a control laser can be used to enhance or even to resolve an apparently inconspicuous hyperfine dip from the Doppler broadened background. This method suffers from the drawback that in this case the hyperfine dip gets broadened.

5 Conclusion

In contrast to the saturation spectroscopic methods [5] we have used two separate laser beams to study the saturation effect. Both the co and counter propagating pump-probe double resonance spectroscopy produces several resonances of sub natural widths in a strongly absorbing medium. These resonances may find various technological applications such as production of miniature atomic clocks to name one. In various phenomena like CPT, EIT [23], quantum information processing optical pumping often plays a very important role. We have carried out a detailed study of various processes leading to the phenomenon of optical pumping.

Through a systematic study of pump probe spectroscopy with the various orientations of the pump and probe beams, we have investigated the effect of optical pumping on the probe absorption profile in presence of a strong pump beam. The strong pump laser transfers atoms from one ground state of the probe to the other ground state resulting in the formation of strong and wide transmission dips across the probe absorption profile. The appreciable widths of these dips may deteriorate the resolution of the sub Doppler features. Following the methods adopted in laser cooling [1] experiments an effort to reduce the optical pumping is made by the use of a hyperfine pumping or repumping laser. The primary function of this laser is to transfer the atoms back from the dark ground state to the excited states from where they are partly transferred into the emission absorption cycle of the pump and probe lasers.

Frequency locking plays a very crucial role in experiments based on the application of laser cooling and trapping. In order to lock the laser to a particular hyperfine transition we normally carry out sub Doppler Lamb dip spectroscopy. However it often becomes very difficult to identify the required hyperfine transmission dip on the broad Gaussian absorption background with the closely spaced hyperfine and crossover transitions [8]. Thus the Gaussian profile has to be subtracted using a balance detector in order to clearly view the hyperfine dip. In this article we suggest a hitherto unattempted method of extracting the faintly resolved hyperfine dips from the Lamb dip spectrum without subtracting the Gaussian background. A strong control laser is used to retrieve the apparently unobtrusive hyperfine dip from the Gaussian background. This makes the hyperfine dip perceptible for efficient frequency locking. The set of experiments reported in this work shows that atoms of different velocity groups can be selectively excited and transferred to a second lower level. The velocity grouping of the atoms may be useful in other experiments where specific velocity atoms need to be investigated.

This work was supported by the BRNS-DAE, Mumbai and the FIST programme of DST, New Delhi.

References

1. H.J. Metcalf, P. van der Straten, *Laser Cooling and Trapping* (Springer, 1999)
2. Y. Sortais, S. Bize, C. Nicolas, A. Clairon, Phys. Rev. Lett. **82**, 3117 (2000)
3. R. Wynands, S. Weyers, Metrologia **42**, S64 (2005)
4. K.B. MacAdam, A. Steinbach, C. Wienman, Am. J. Phys. **60**, 1098 (1992)
5. M.D. Levenson, S.S. Kano, *Introduction to Nonlinear Laser Spectroscopy* (Academic, New York, 1988)
6. Luo Caiyan, S. Kroll, L. Sturesson, S. Svanberg, Phys. Rev. A **53**, 1668 (1996)
7. D.A. Steck, rubidium 87 D line data, rev 1.6, `http://steck.us/alkalidata` (2003)
8. H.R. Schlossberg, A. Javan, Phys. Rev. **150**, 267 (1966)
9. S. Mandal, P.N. Ghosh, Phys. Rev. A **45**, 4990 (1992)
10. D. Bhattacharyya, B.K. Dutta, B. Ray, P.N. Ghosh, Chem. Phys. Lett. **389**, 113 (2004)
11. D.A. Smith, I.G. Hughes, Am. J. Phys. **72**, 631 (2004)
12. M.S. Feld, M.M. Burns, T.U. Kühl, P.G. Pappas, Opt. Lett. **5**, 79 (1980)
13. A.M. Akulshin, V.A. Sautenkov, V.L. Velichansky, A.S. Zibrov, M.V. Zverkov, Opt. Commun. **77**, 295 (1990)
14. V. Wong, R.W. Boyd, C.R. Stroud, R.S. Vennink, A.N. Marino, Phys. Rev. A **68**, 012502 (2003)
15. D. Fulton, S. Shepherd, R.R. Moseley, B.D. Sinclair, M.H. Dunn, Phys. Rev. A **52**, 2302 (1995)
16. M. Stahler, R. Wynands, S. Knappe, J. Kitching, L. Hollberg, A. Taichenachev, V. Yudin, Opt. Lett. **27**, 1472 (2002)
17. J. Kitching, L. Hollberg, S. Knappe, R. Wynands, Electron. Lett. **37**, 1449 (2001)
18. G. Jundt, G.T. Purves, C.S. Adams, I.G. Hughes, Eur. Phys. J. D **27**, 273 (2003)
19. Y. Zhu, Phys. Rev. A **45**, R6149 (1992)
20. J. Ye, S. Swartz, P. Jungner, J.L. Hall, Opt. Lett. **21**, 1280 (1996)
21. T. Petelski, M. Fattori, G. Lamporesi, J. Stuhler, G.M. Tino, Eur. Phys. J. D **22**, 279 (2003)
22. S. Chakrabarti, A. Pradhan, A. Bandyopadhyay, A. Ray, B. Ray, N. Kar, P.N. Ghosh, Chem. Phys. Lett. **399**, 120 (2004)
23. S. Chakrabarti, A. Pradhan, B. Ray, P.N. Ghosh, J. Phys. B: At. Mol. Opt. Phys. **38**, 4321 (2005)